*Scientific paper*

# Properties of the $(Y_{0.75}Gd_{0.25})_2O_3:Eu^{3+}$ Scintillating Nanopowder

**Željka Andrić,[a] Radenka Krsmanović,[a] Miodrag Mitrić,[a] Zoran Marković,[a] Bruno Viana[b] and Miroslav D. Dramićanin[a]***

[a] *Institute of Nuclear Sciencies "Vinča," P.O. Box 522, 11000 Beograd, Serbia*

[b] *Laboratoire de Chimie de la Matière Condensée de Paris (ENSCP), CNRS UMR 7574 11, rue P et M Curie, 75231 Paris cedex 05, France*

** Corresponding author: E-mail: dramican@vin.bg.ac.yu*

*Received: 09-07-2007*

## Abstract

Yttrium-gadolinium-oxide phosphors are regarded promising host for many important optical applications, for example in medical diagnostic X-ray systems and plasma displays. In this work, we investigated the procedure for $(Y_{0.75}Gd_{0.25})_2O_3:Eu^{3+}$ nanopowder synthesis using polymer complex solution (PCS) method based on polyethylene glycol (PEG) as fuel. Detailed information, on both the structure and luminescence, are obtained using X-ray powder diffraction, electron microscopy and luminescence spectroscopy. The synthesized powder consists of nanoparticles of about 36 nm in size, and has excellent structural ordering in cubic bixbyte structure (space group Ia3). Unit cell parameter, ionic coordinates, crystal coherence size and microstrains are determined from Rietveld analysis. Luminescence emission measurements show characteristic transition of the trivalent europium ion incorporated into insulating host. Splitting of the Stark components of the $^7F_1$ manifold is presented. $^5D_0$, $^5D_1$ and $^5D_2$ decay time values are measured to obtain information on different kinetic processes occurring for these three emitting levels.

**Keywords:** Combustion synthesis, yttrium-gadolinium oxide, PEG, luminescence spectroscopy.

## 1. Introduction

The $Ln_2O_3$ rare-earth oxides in the lanthanide series, or sesquioxides, have been of particular interest to the research community over the last century. The rare-earth oxides, being the most widespread lanthanide compounds, are commonly utilized as a catalyst for the synthesis of many other 4f-materials. Phosphors based on $Eu^{3+}$ doped rare-earth (RE) sesquioxides such as yttrium, lanthanum and gadolinium are important materials with numerous applications in different fields. In particular, $Eu^{3+}$ doped $(Y, Gd)_2O_3$ is well-known luminescent material widely used to provide red light emission for modern optoelectronic devices.[1–5]

Nanoparticles have sparked intense interest expecting that this range of materials dimension will yield size-dependant properties. Both physical and chemical properties vary with size and the use of ultrafine particles clearly represents a fertile field of materials research. During the past decade, optical properties of nanosized materials have attracted considerable interest. Stronger luminescence emission in nanocrystalline materials compared to bulk materials and modification of radiative lifetime have been reported.[6] It is shown that doping uniformity and phase purity are easier to achieve with nanomaterials. Internal scattering in nanomaterial is reduced as the size of the phosphor particles is much smaller than the wavelength of the visible light. Moreover, in nanophosphors the dopant concentrations can be increased as the quenching effect due to the energy transfer between emission centers is greatly reduced.

Common methods for preparation of nanophosphors are sol-gel, precipitation, co-precipitation, emulsion, combustion, spray pyrolysis, etc. It is known that several synthetic procedures could facilitate formation of C-type stable solid solutions for all $Y_2O_3$–$Gd_2O_3$ compositions.[7, 8, 9] We present here polymer complex solution method – a variation of combustion technique, as synthesis technique for nanocrystalline $Y_{0.75}Gd_{0.25}O_3$: $Eu^{3+}$ (3 at % of Eu). This method is based on the fact that the reaction of polymer complex solution is very fast and intense combustion reaction where polymer substance (in our case polyethyle-

ne glycol – PEG) is used as a fuel. In this process large amount of gaseous products and heat are generated resulting in very porous material. The characterization is done with XRD, SEM, TEM and luminescence spectrometry and obtained results presented in this paper.

## 2. Results and Discussion

XRD analysis of $(Y_{0.75}Gd_{0.25})_2O_3$ sample confirms that the powder crystallizes in cubic bixbyte structure (space group Ia3), same structure of the starting materials $Y_2O_3$ and $Gd_2O_3$. In this structural type cations occupy two different crystallographic positions 8b (¼, ¼, ¼) with point symmetry $\bar{3}$ ($S_6$, $C_{3i}$) and 24d ($x$, 0, ¼) with point symmetry 2 ($C_2$). Both cations are octahedral coordinated. The oxygen ion, in the general 48e position, is tetrahedrally surrounded.[10] Elementary cell is body centered with 16 formulae units. Measured XRD pattern together with final Rietveld plot is given in Figure 1, and relevant data are reported in Table 1.

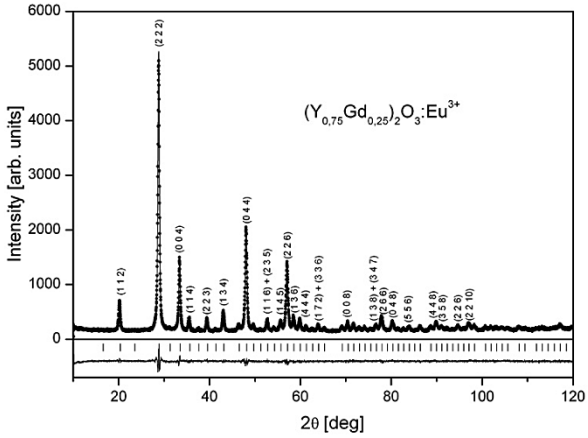


**Figure 1** The observed (crosses), calculated (solid line) and difference XRD patterns for $(Y_{0.75}Gd_{0.25})_2O_3:Eu^{3+}$ nanopowder.

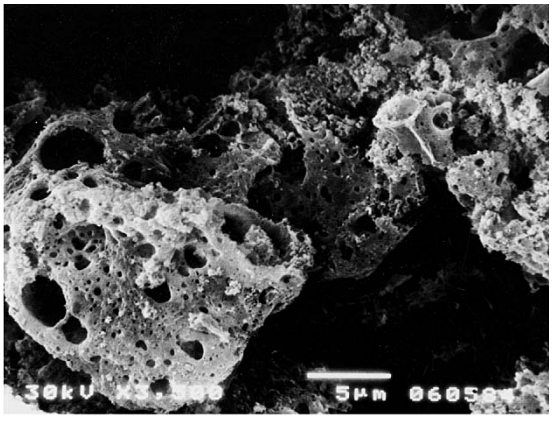


**Figure 2** Typical SEM image of $(Y_{0.75}Gd_{0.25})_2O_3:Eu^{3+}$ powder.

SEM observations revealed the nature of the combustion synthesis: at micron-level our sample has a porous, sponge-like morphology, with lot of pores and voids, as can be seen in one representative SEM image in Figure 2. The presence of pores and voids results from the large quantity of escaping gases during combustion reaction.

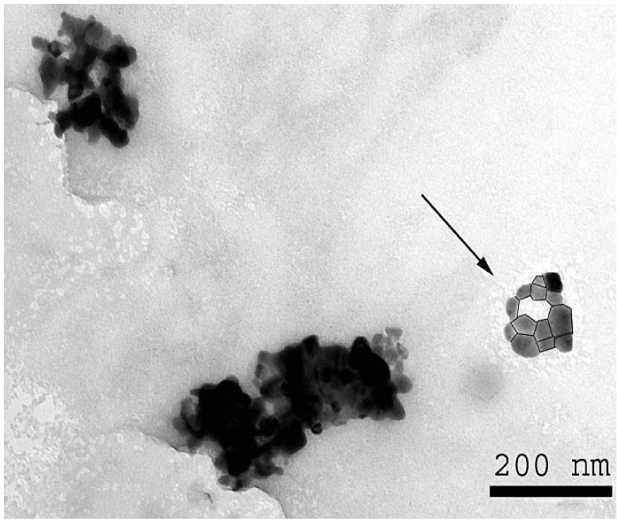


**Figure 3** TEM image of one region containing agglomerates of $(Y_{0.75}Gd_{0.25})_2O_3:Eu^{3+}$ nanoparticles. To make them more visible we delineated the contours of nanoparticles in the agglomerate indicated with an arrow.

Morphology and particle sizes are further checked with TEM (Figure 3). At nanometer-level phosphor particles have irregularly spherical or elliptical morphology and form agglomerates. The particle sizes are in the range of 25 to 50 nm. Probably the final, post-synthesis calcination is the reason for some inter-particle sintering (see arrowed agglomerate in Figure 3 and the formation of larger agglomerates.

Figure 4 shows the fluorescence decay curves of the $^5D_0$ and $^5D_1$ emitting levels obtained under excitation at 21598 $cm^{-1}$ (463 nm) ($\lambda_{em}(^5D_0)$ = 16345 $cm^{-1}$ (611.8 nm); $\lambda_{em}(^5D_1)$ = 18762 $cm^{-1}$ (533 nm)). In both cases, fluorescence decay profiles could be adjusted by a single-exponential function and the obtained lifetimes are given in the Table 2. The decay profile of $^5D_2$ emitting level (excitation at 21598 $cm^{-1}$ (463 nm), emission at 20000 $cm^{-1}$ (500 nm)) has a complex profile and can be approximated with

**Table 1** Selected parameters obtained after Rietveld analysis of XRD patterns for $(Y_{0.75}Gd_{0.25})_2O_3:Eu^{3+}$.

| Cell parameter $a$ | $Y^{3+}$, $Gd^{3+}$ | | | | Microstrain | Crystal coherence size |
|---|---|---|---|---|---|---|
| [Å] | $x$ | $x$ | $y$ | $z$ | $\Delta a/a$ [%] | [nm] |
| 10.6784 (1) | –0.0313 (1) | 0.3923 (5) | 0.1523 (4) | 0.3829 (6) | 0.081 (8) | 35.6 (4) |

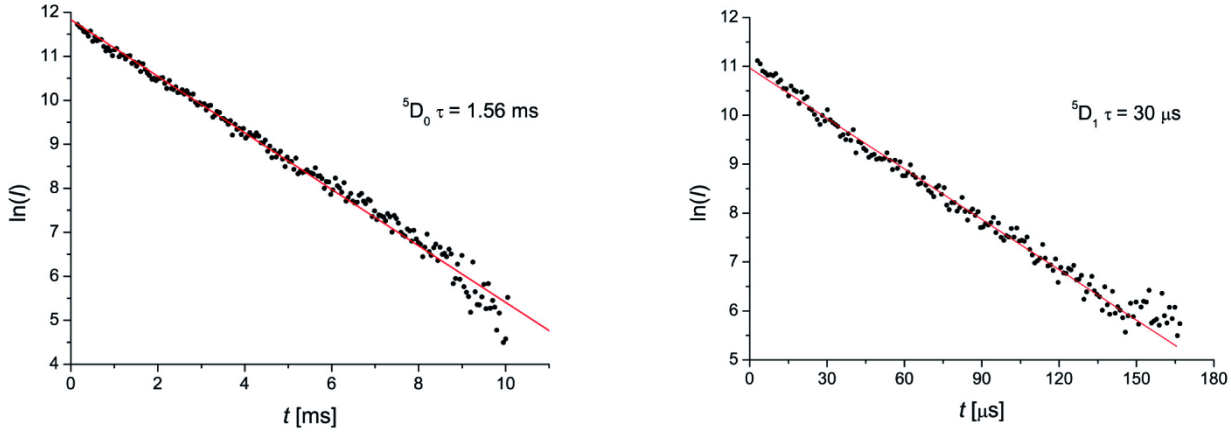


**Figure 4** Fluorescence decay profile for $^5D_0$ (τ = 1.56 ms) and $^5D_1$ (τ = 30 μs) levels.

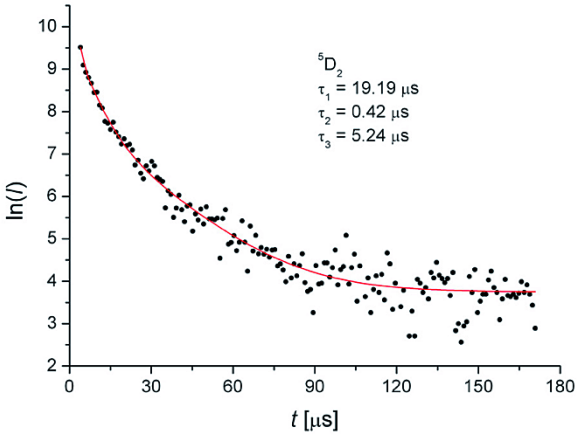


**Figure 5** Fluorescence decay profile for $^5D_2$ level.

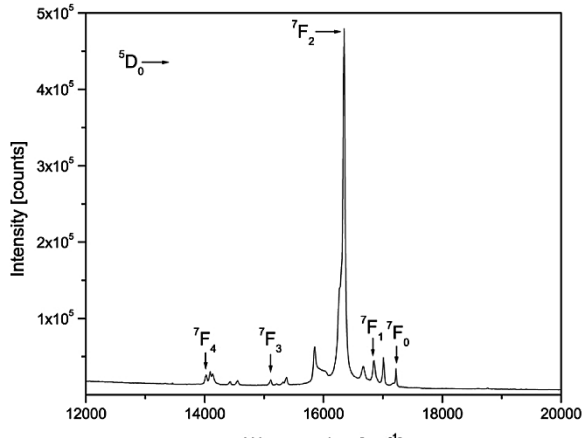


**Figure 6** Luminescence spectra of $(Y_{0.75}Gd_{0.25})_2O_3$:$Eu^{3+}$ obtained with 200 μs delay time.

three exponential functions with decay times of 19.2, 5.4 and 0.4 μs. (Figure 5). Further experiments are in progress to describe processes responsible for behavior. Quite high values are obtained for $^5D_1$ and $^5D_2$ lifetimes. In this case, cross relaxation effects, which is the major process involved in the reduction of the trivalent europium $^5D_{1,2}$ lifetimes, seems to be weak. This indicates homogeneous distribution of $Eu^{3+}$ ions in nanoparticles.

Luminescence emission spectra of $(Y_{0.75}Gd_{0.25})_2O_3$:$Eu^{3+}$ nanopowders are presented on Figures 6–8. Measurements are performed with different time delays after the laser pulse in order to observe the contributions of different emitting levels. Luminescence spectrum obtained with the 200 μs delay time is presented in Figure 6. Taking into account measured values of $^5D_1$ and $^5D_2$ lifetimes (30 μs and 19 μs, respectively), the observed features primarily corresponds to $^5D_0$ emission. In this figure, five characteristic bands centered at around 17223, 16853, 16345, 15860 and 14250 $cm^{-1}$ associated to $^5D_0 \rightarrow {}^7F_i$ ($i$ = 0, 1, 2, 3 and 4) spin forbidden f–f transitions are observed. The $^5D_0 \rightarrow {}^7F_1$ transition is the parity-allowed magnetic dipole transition (ΔJ = 1) and its intensity does not vary with the host. On the contrary, the $^5D_0 \rightarrow {}^7F_2$ electric dipole transition (ΔJ = 2) is very sensitive to the local environment

**Table 2** Selected parameters obtained after luminescence measurements for $(Y_{0.75}Gd_{0.25})_2O_3$:$Eu^{3+}$.

| $^5D_0 \rightarrow {}^7F_0$ $C_2$ site [$cm^{-1}$] | $^5D_0 \rightarrow {}^7F_1$ $C_2$ site [$cm^{-1}$] | $^5D_0 \rightarrow {}^7F_1$ $S_6$ site [$cm^{-1}$] | *R* | ΔE [$cm^{-1}$] | τ($^5D_0 \rightarrow {}^7F_2$) [ms] | τ($^5D_{10} \rightarrow {}^7F_2$) [μs] | τ($^5D_{20} \rightarrow {}^7F_2$) [μs] |
|---|---|---|---|---|---|---|---|
| 17223.3 | 17011.3<br>17169.2<br>16673.6 | 16853.8 | 0.0997 | 337.7 | 1.56 | 30 | 19.2, 5.4 and 0.4 |

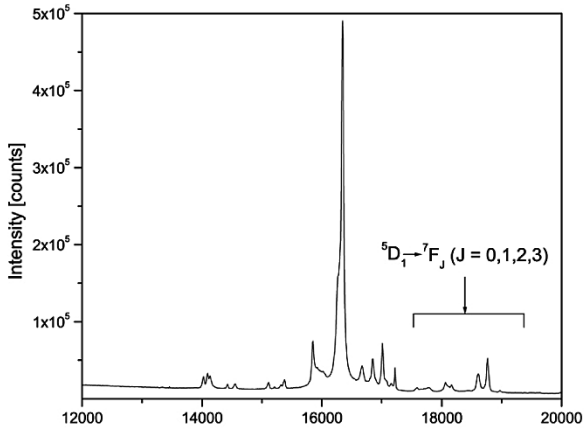


**Figure 7** Luminescence spectra of $(Y_{0.75}Gd_{0.25})_2O_3:Eu^{3+}$ obtained with 30 μs delay time.

around $Eu^{3+}$ ion, and its intensity depends on the symmetry of the crystal field around $Eu^{3+}$ ion.

The symmetry ratio of the integrated intensity of the $^5D_0 \rightarrow ^7F_2$ and $^5D_0 \rightarrow ^7F_1$ transitions, i.e. R = I ($^5D_0 \rightarrow ^7F_1$) / I ($^5D_0 \rightarrow ^7F_2$), is considered to be the indicator of the symmetry of the coordination environment around the $Eu^{3+}$ ion (see Table 2). Stark components of the $^7F_1$ manifold are clearly visible and their values, together with values of maximum splitting $\Delta E$, are given in Table 2.

Luminescence spectra obtained with 30 μs and 30 ns time delay are presented in Figure 7 and Figure 8, respectively. In the former both the $^5D_2$ and $^5D_1$ levels are observed, while in the later the faster kinetics is favoured ($^5D_2$ level). From these measurements the $^5D_i \rightarrow ^7F_j$ transitions are identified and labeled on Figures 6–8.

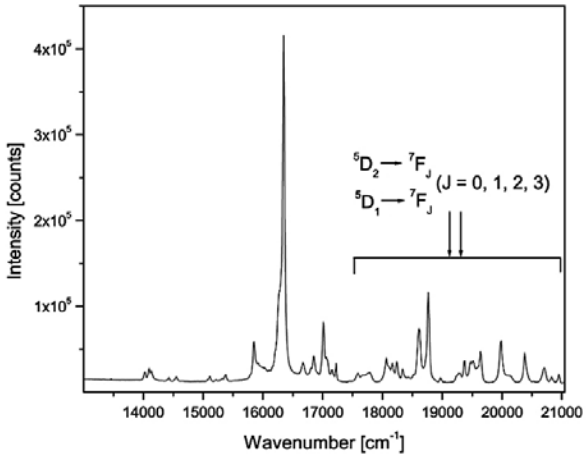


**Figure 8** Luminescence spectra of $(Y_{0.75}Gd_{0.25})_2O_3:Eu^{3+}$ obtained with 30 ns delay time.

## 3. Conclusions

Nanocrystalline, pure phase of yttrium-gadolinium mixed oxide ($(Y_{0.75}Gd_{0.25})_2O_3$) has been successfully synthesized by a complex polymer solution method, employing PEG as fuel. Well crystallized particles have size of about 36 nm. The characterization is done by XRD, SEM and TEM, and luminescence spectroscopy and the main conclusions are summarized as follows:

(*i*) Data obtained from Rietveld analysis of XRD patterns and luminescence measurements demonstrated that perfect mixing of yttrium oxide and gadolinium oxide has been accomplished for the studied oxide composition: $(Y_{0.75}Gd_{0.25})_2O_3:Eu^{3+}$. (*ii*) The TEM observations indicate that irregularly spherical nanocrystallites are the main constitute elements of μm-size, very porous regions observed at SEM. The average particle diameter determined from TEM images is about 36 nm that is consistent with the mean crystallite size determined from XRD data. (*iii*) When excited into $^5D_2$ absorption band nanopowder exhibit strong red luminescence typical for trivalent europium ion. Different delay times after excitation provided luminescence spectra which favors luminescence from different $^5D_J$ (J = 0, 1, 2) levels, and enable detection of all transition present in the visible spectral range. This is in contrast to bulk phosphor where 3 at % concentration of Eu were sufficient to quench higher level emission (i.e. $^5D_J \rightarrow ^7F$, J > 0).[11] Taking into account also quite high values obtained for $^5D_1$ and $^5D_2$ lifetime, of 30 μs and 19 μs, respectively, we may point to the existence of inefficient cross relaxation processes and homogeneous distribution of $Eu^{3+}$ ions in nanoparticles. (iv) The $^5D_0$ lifetime of 1.56 ms is much higher than those found in bulk $Y_2O_3$ and $Gd_2O_3$ (respectively 1 and 1.1 ms[12]) indicating the possibility of production of material with higher emission yield. The explanation for observed high value of $^5D_0$ lifetime can be found in a refractive index variation in effective medium.[6]

## 4. Experimental

Nanocrystalline $(Y_{0.75}Gd_{0.25})_2O_3:Eu^{3+}$ (3 at % of Eu) was prepared by polymer complex solution (PCS) method. The initial material – $Y_2O_3$, $Gd_2O_3$ and $Eu_2O_3$ were dissolved in hot nitric acid. In obtained solutions of stoichiometric quantities of Y, Gd and Eu-nitrate PEG was added in 1:1 mass ratio to used oxides. After forming metal-PEG solutions and stirring at 80 °C, metal-PEG solid complex was formed. Complex is combusted at 800 °C in air and then calcinated at same temperature for 2h.

X-ray diffraction measurements are obtained with Philips PW 1050 instrument, using Ni filtered Cu $K\alpha_{1,2}$ radiation. Diffraction data were recorded in 2θ range from 10° to 120° counting for 15 s in 0.02° steps. Structure analysis was performed using KOLARIE computer software based on a Rietveld full profile refinement method.

Particle morphology and agglomeration state of the synthesized powders were observed with scanning electron microscopy (SEM – JEOL: JKSM-5300). Particle size of $(Y_{0.75}Gd_{0.25})_2O_3:Eu^{3+}$ nanoparticles were determined

by transmission electron microscopy – TEM (Phillips CM100 instrument). SEM and TEM specimens were prepared with standard powder preparation techniques.

The emission spectra have been collected at room temperature after excitation into the $^7F_0 \rightarrow {}^5D_2$ absorption band. The excitation source was an Optical Parametric Oscillator (O.P.O.) pumped by the third harmonic of the Nd:YAG laser. The emission has been analyzed using HR250 monochromator (Jobin-Yvon) and then detected by an ICCD camera (Princeton Instrument). The emissions are recorded with the following delay time after the laser excitation: 30 ns, 30 ms and 200 ms, in order to limit contributions from different emitting levels. Lifetime measurements have been recorded under pumping by the O.P.O. at 463 nm at room temperature. $^5D_2$, $^5D_1$ and $^5D_0$ decay time values provide information on different kinetic processes occurring for these three emitting levels.

## 5. Acknowledgements

This work was supported by the Ministry of Science of the Republic of Serbia (Project 142066).

## 6. References

1. B. Bihari, H. Eilers, B. Tissue, *J. Lumin*., 1997, *75*, 1–10.
2. R. Schmechel, M. Kennedy, H. von Seggem, H. Winkler, M. Kolbe, R. Fisher, L. Xaomao, A. Benker, M. Winterer, H. Hahn, *J. Appl. Phys*., 2001, *89*, 1679–1688.
3. P. Majewski, M. Rozumek, H. Schluckwerder, F. Aldinger, *Int. J. Inorganic Mater*., 2001, *3*, 1343–1344.
4. Garcia-Murillo, C. Luyer, C. Garapon, C. Dujardin, E. Bernstein, C. Pedrini, J. Mugnier, *Opt. Mater*., 2002, *19*, 161–168.
5. W. Jungowska, *J. Thermal Anal. Calorimetry*, 2000, *60*, 193–197.
6. R. S. Meltzer, S. P. Feofilov, R. Tissue and H. B. Yuan, *Phys. Rev. B.,* 1999, *60*, 14012–14015.
7. G. Adachi, N. Imanaka, *Chem. Rev.*, 1998, *98*, 1479–1514.
8. N. Hirosaki, S. Ogata and C. Kocer, *J. Alloys Compds*., 2003, *351,* 31–34.
9. A. Chroneos and G. Busker, *Acta Chim. Slov.,* 2005, *52*, 417–421.
10. M. Mitric, P. Onnerud, D. Rodic, R. Tellgren, A. Szytula, M. Lj. Napijalo, *J. Phys. Chem. Solids*, 1993, *54*, 967–972.
11. M. Buijs, A. Meyerink and G. Blasse, *J. Lumin.* 1987, *37*, 9–20.
12. O. Pons Y Moll, A. Huignard, E. Antic-Fidancev, P. Aschehoug, B. Viana, E. Millon, J. Perriere, C. Garapon, J. Mugnier, *J. Lumin.* 2000, 14012–14016.

## Povzetek

Itrij-gadolinijevi oksidi so obetavni materiali za številne pomembne aplikacije v optiki, kot so na primer sistemi za Rentgensko medicinsko diagnostiko in plazemski ekrani. V tem prispevku je opisan postopek za sintezo nanoprahov $(Y_{0.75}Gd_{0.25})_2O_3:Eu^{3+}$ z uporabo metode kompleksne raztopine polimerov (PCS) na osnovi polietilenglikola (PEG) kot goriva. Podatke o strukturi in luminiscenci sintetiziranega materiala smo dobili z X-žarkovno difrakcijo prahov, elektronsko mikroskopijo in luminiscenčno spektroskopijo. Sintetizirani material sestavljajo nanodelci velikosti 30 nm s kubično biksbitno strukturo (prostorska grupa Ia3). Parametre osnovne celice, ionske kordinate, koherenčno dolžino in mikronapetosti smo določili z Rietveldovo analizo. Meritve luminiscence so pokazale energijske prehode trivalentnih ionov evropija, značilne za koordinacijo sosednjih atomov v sintetiziranem nanoprahu. Izmerili smo razpolovne dobe $^5D_0$, $^5D_1$ in $^5D_2$ stanj in dobili podatke o različnih kinetičnih procesih za tri emisijske nivoje.